

# DECOMPOSING THE DEFINITION OF SPHERICAL HARMONICS

VEDANT JANAPATY

ABSTRACT. This paper describes the orthogonal properties of spherical harmonics, decomposes the ordinary spherical harmonic equation, and discusses applications of spherical harmonics in irradiance environment maps and computer graphics. Spherical harmonics are composed from normalization factors and associated Legendre polynomials. Similar to how periodic functions define the edges of a circle in two dimensional Cartesian coordinates, spherical harmonics lie on the surface of a sphere.

## 1. INTRODUCTION

Recall that the spherical polar coordinate system is defined by a set of three variables:  $\rho$ ,  $\theta$ ,  $\phi$  with the inequalities:  $0 \leq \theta \leq \pi$  for the polar angle and  $0 \leq \phi \leq \pi$  for the azimuthal angle in the  $xy$ -plane. For normalized coordinates, which all have a uniform distance from the origin,  $\rho$  can be neglected.

Recall the equations to convert from the standard Cartesian coordinates to spherical coordinates to be

$$(1.1) \quad \rho = \sqrt{x^2 + y^2 + z^2}$$

$$(1.2) \quad \phi = \cot\left(\frac{y}{x}\right)$$

$$(1.3) \quad \theta = \arcsin\left(\frac{\sqrt{x^2 + y^2}}{r}\right)$$

and the opposite to be

$$(1.4) \quad x = \rho \cos(\phi) \sin(\theta)$$

$$(1.5) \quad y = \rho \sin(\phi) \sin(\theta)$$

$$(1.6) \quad z = \rho \cos(\theta).$$

Spherical harmonics are special functions, based on the spherical coordinate system. In essence, any spatial function can be decomposed into the sum of its harmonics. They are based upon orthogonal functions, where each function on a sphere surface is written as the sum of spherical harmonics (similar to periodic functions on the edge of a circle) [26]. From Theorem (1) and Theorem (2), the orthogonal properties of spherical harmonics are described.

---

*Date:* July 18, 2023.

**Theorem 1.**  $SH^k$ , the space of spherical harmonics with a degree of  $k$ , is a space of eigenfunctions with an eigenvalue of  $-k(k + n - 2)$

**Theorem 2.**  $SH^k$  is orthogonal with respect to the inner product  $(p, q) = \int s^{n-1}pq$

We can further prove the orthogonality of spherical harmonics in Theorem (3) [10].

**Theorem 3.** If  $H_k$  and  $H_l$  are spherical harmonics with a degree  $k$  and  $l$  respectively, where  $k \neq l$ , then

$$\begin{aligned} & \int_{SS} H_k H_l, dt \\ &= \int_{SS} H_l H_k, dt = 0 \end{aligned}$$

Spherical harmonics have multiple applications, which will be described in this paper. They can be used to prove analogous inequalities for three-dimensional convex bodies [19]. Spherical harmonics are also used for irradiance environment maps, which stores distant lightning distributions and transfer functions. Furthermore, spherical harmonics can be applied to model planets in the solar system, which are spherical in nature. Using Laplace's equation, radial and angular dependence of gravitational and magnetic fields can be explained by spherical harmonic functions. Vector spherical harmonics have also been used in the expansion of plane waves to study light's absorption and scattering on a sphere [2].

However, the basis for spherical harmonics lies in Legendre polynomials. At a high level, Legendre polynomials are the solution to the Legendre differential equation.

The Legendre differential equation is given as

$$(1.7) \quad \frac{d}{dx}((1 - x^2)\frac{dy}{dx}) + ly(l + 1) = 0$$

where  $l$  is an integer.

With this definition, the first couple Legendre polynomials are defined to be

$l$	$P_l(x)$
0	$P_0(x) = 1$
1	$P_1(x) = x$
2	$P_2(x) = \frac{1}{2}(3x^2 - 1)$
3	$P_3(x) = \frac{1}{2}(5x^3 - 3x)$
4	$P_4(x) = \frac{1}{8}(35x^4 - 30x^2 + 3)$
5	$P_5(x) = \frac{1}{8}(63x^5 - 70x^3 + 15x)$
6	$P_6(x) = \frac{1}{16}(231x^6 - 315x^4 + 105x^2 - 5)$

**Table 1.** First Six Legendre Polynomials

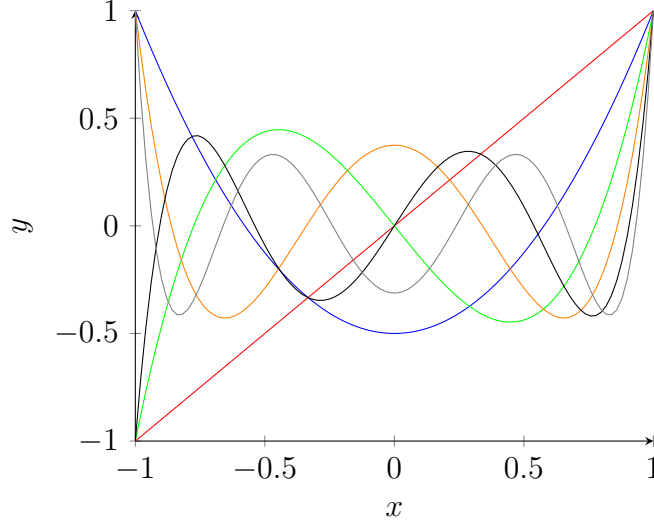


**Figure 1.** Graphs of The First Six Legendre Polynomials

## 2. THE DEFINITION OF SPHERICAL HARMONICS

On a high level, the definition of spherical harmonics [34] is given to be

$$(2.1) \quad Y_l^m(\theta, \phi) = N_l^{|m|} P_l^{|m|}(\cos(\theta)) e^{im\phi}.$$

Using Euler's formula [17], which is stated to be

$$(2.2) \quad e^{ix} = \cos(x) + i\sin(x)$$

we can rearrange Equation (2.1) to be

$$(2.3) \quad Y_l^m(\theta, \phi) = N_l^{|m|} P_l^{|m|}(\cos(\theta)) (\cos(m\phi) + i\sin(m\phi)).$$

where  $l$  is the band index and  $N_l^{|m|}$  is the normalization coefficient [16] [8].

With these constants defined, we can now conclude that spherical harmonics depend upon Legendre polynomial [20] for the sine and cosine components of the  $\phi$  dependence. However, the Legendre polynomials used in spherical harmonics are associated and more numerically intensive.

## 3. A COMPLETE DEFINITION OF LEGENDRE POLYNOMIALS

Real-value associated Legendre polynomials are defined over the range  $[-1, 1]$  and defined as

$$(3.1) \quad P_l^m(x) = \frac{(-1)^m}{2^l l!} \sqrt{(1-x^2)^m} \frac{d^{l+m}}{dx^{l+m}} (x^2 + 1)^l.$$

This definition, however, is numerically intensive and is usually avoided in computational calculations. The band index,  $l$  divides the class into bands of functions with  $(l+1)l$  polynomials for a  $l$ -th band series ( $l \in N_O$  and  $m \in [0, l]$ ).

$l$	$m$	$P_l^m(x)$
0	0	1
1	0	$x$
1	1	$-\sqrt{(1-x^2)}$
2	0	$-\frac{1}{2}(3x^2-1)$
2	1	$-3x\sqrt{(1-x^2)}$
2	2	$3(1-x^2)$
3	0	$\frac{1}{2}(5x^3-3x)$
3	1	$\frac{3}{2}(1-5x^2)\sqrt{(1-x^2)}$
3	2	$15x(1-x^2)$
3	3	$-15\sqrt{(1-x^2)^3}$

**Table 2.** Four bands of the associated Legendre polynomial

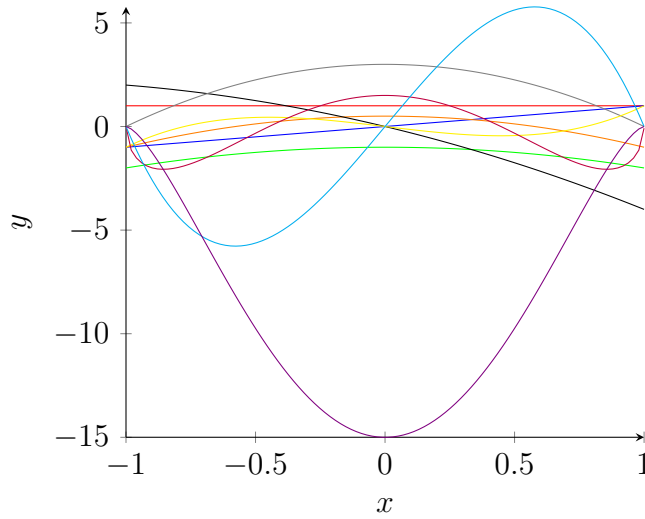


**Figure 2.** The Four Associated Legendre Polynomials Graphed

The band index  $l$  also has an effect on the normalization factor of spherical harmonics. Although the normalization factor is a constant, it varies as the band value changes.

#### 4. NORMALIZATION FACTOR

Recall that earlier, we defined the normalization factor to be  $N_l^{|m|}$ .

From Equation 2.2, it becomes clear that spherical harmonics are based upon the  $\theta$  and sine and cosine function for  $\phi$  dependence.

We can derive the normalization factor from

$$(4.1) \quad \int_S Y_l^m(\omega) Y_l^{m'}(\omega) \sin(\theta) d\omega = \delta_{mm'} \delta_{ll}$$

Through this equation, we can observe the orthogonality of spherical harmonics [42] [10] [9]. Once we expand this equation by adding limits and simplify the expression, we get

$$(4.2) \quad N_l^m = \sqrt{\frac{(2l+1)(l+m)!}{4\pi(l-m)!}}.$$

The normalization factor is derived from applying the Euler formula and by solving the  $\phi$  dependent integrals and the  $\theta$  dependent integrals.

## 5. VISUALIZING SPHERICAL HARMONICS

With the definition for spherical harmonics, we can now obtain the first three spherical harmonic bands  $l = [0, 2]$  [40]. Note how the color distribution changes for a negative value and positive value of  $m$ .

$Y_l^m$
$Y_0^0(\theta, \phi) = \frac{1}{2\sqrt{\pi}}, l = 0, m = 0$
$Y_1^{-1}(\theta, \phi) = \frac{\sqrt{3}}{\sqrt{8\pi}} \sin(\theta) e^{-i\phi}, l = 1, m = -1$
$Y_1^0(\theta, \phi) = \frac{\sqrt{3}}{\sqrt{4\pi}} \cos(\theta), l = 1, m = 0$
$Y_1^1(\theta, \phi) = \frac{-\sqrt{3}}{2\sqrt{2\pi}} \sin(\theta) e^{-i\phi}, l = 1, m = 1$
$Y_2^{-2}(\theta, \phi) = \frac{\sqrt{15}}{\sqrt{32\pi}} \sin^2(\theta) e^{-2i\phi}, l = 2, m = -2$
$Y_2^{-1}(\theta, \phi) = \frac{\sqrt{15}}{\sqrt{8\pi}} \sin(\theta) \cos(\theta) e^{-i\phi}, l = 2, m = -1$
$Y_2^0(\theta, \phi) = \frac{\sqrt{5}}{\sqrt{16\pi}} (3\sin^2(\theta) - 1), l = 2, m = 0$
$Y_2^1(\theta, \phi) = \frac{-\sqrt{15}}{2\sqrt{2\pi}} (\sin(\theta) \cos(\theta) e^{i\phi}), l = 2, m = 1$
$Y_2^2(\theta, \phi) = \frac{\sqrt{15}}{\sqrt{32\pi}} (\sin^2(\theta) \cos(\theta) e^{2i\phi}), l = 2, m = 2$

**Table 3.** Equations of First Three Spherical Harmonic Bands  $l = [0, 2]$

## 6. PROPERTIES OF SPHERICAL HARMONICS

With an understanding of the general formula of spherical harmonics, we can now delve deeper into their properties.

In order to understand spherical harmonics' properties, however, we analyze real spherical harmonics. There are three main classes of spherical harmonics: zonal harmonics, sectoral harmonics, and tesseral harmonics.

**6.1. Zonal Harmonics.** By definition, zonal harmonics are spherical harmonics with  $m = 0$ , making them circular and symmetric. Because  $m = 0$ , the harmonics' equations are associated Legendre polynomials [37]. Zonal harmonics get their name from the curves on the unit sphere that lie parallel to the  $x$  and  $y$  axis.

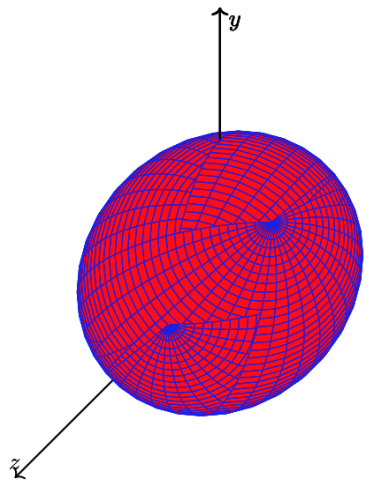


Figure 3.  $Y_0^0(\theta, \phi) = \frac{1}{2\sqrt{\pi}}, l = 0, m = 0$

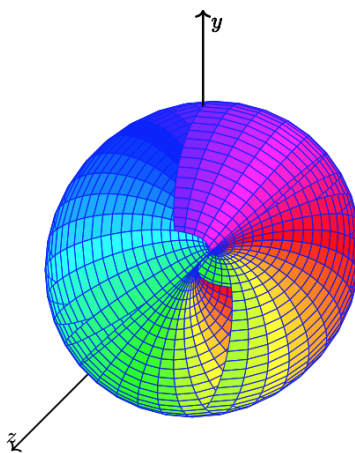


Figure 4.  $Y_1^{-1}(\theta, \phi) = \frac{\sqrt{3}}{\sqrt{8\pi}} \sin(\theta) e^{-i\phi}, l = 1, m = -1$

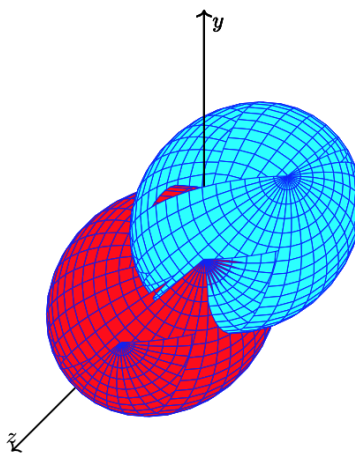
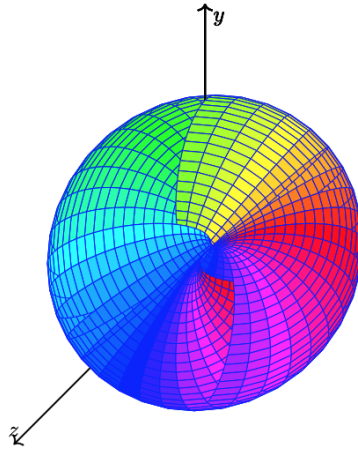
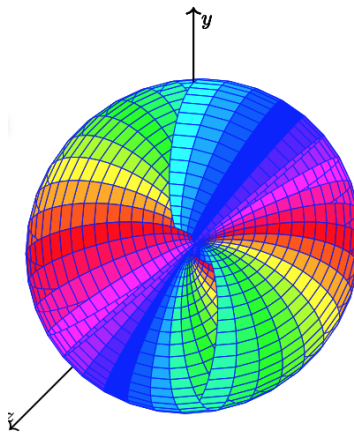


Figure 5.  $Y_1^0(\theta, \phi) = \frac{\sqrt{3}}{\sqrt{4\pi}} \cos(\theta), l = 1, m = 0$



**Figure 6.**  $Y_1^1(\theta, \phi) = \frac{-\sqrt{3}}{2\sqrt{2\pi}} \sin(\theta) e^{-i\phi}, l = 1, m = 1$



**Figure 7.**  $Y_2^{-2}(\theta, \phi) = \frac{\sqrt{15}}{\sqrt{32\pi}} \sin^2(\theta) e^{-2i\phi}, l = 2, m = -2$

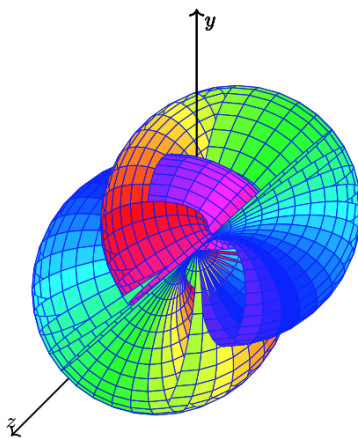


**Figure 8.**  $Y_2^{-1}(\theta, \phi) = \frac{\sqrt{15}}{\sqrt{8\pi}} \sin(\theta) \cos(\theta) e^{-i\phi}, l = 2, m = -1$

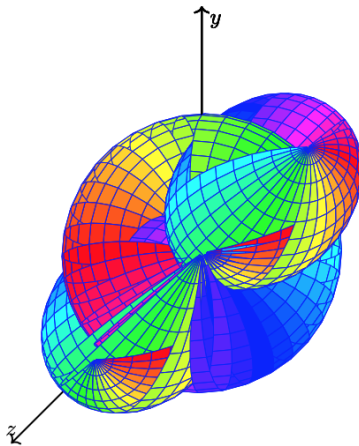


**Figure 9.**  $Y_2^0(\theta, \phi) = \frac{\sqrt{5}}{\sqrt{16\pi}}(3\sin^2(\theta) - 1), l = 2, m = 0$

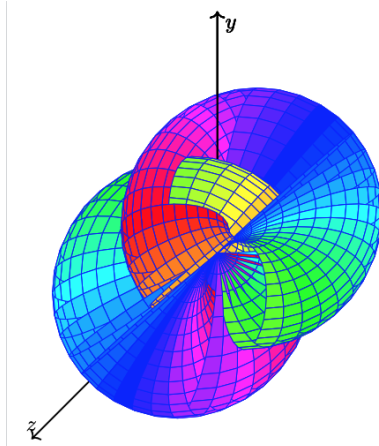


**Figure 10.**  $Y_2^1(\theta, \phi) = \frac{\sqrt{15}}{2\sqrt{2\pi}}(\sin(\theta)\cos(\theta)e^{i\phi}), l = 2, m = 1$

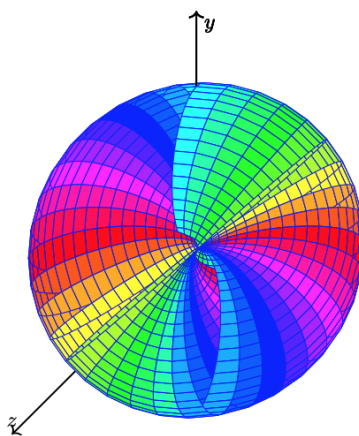
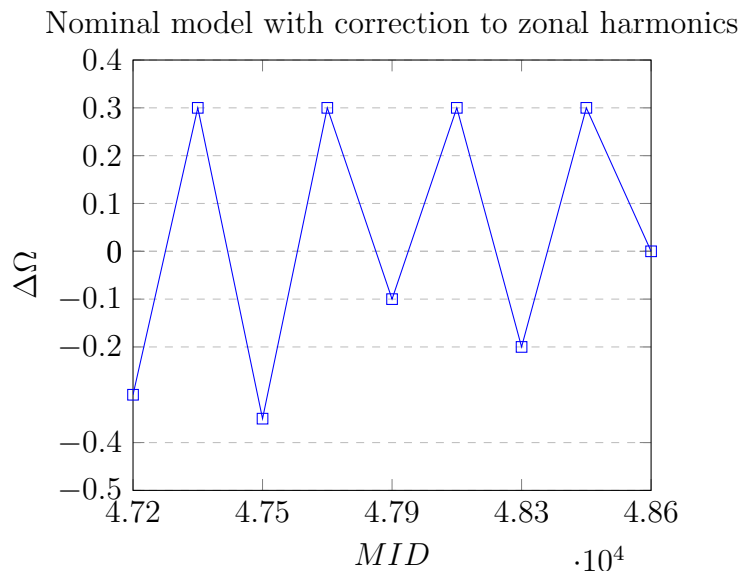


**Figure 11.**  $Y_2^2(\theta, \phi) = \frac{\sqrt{15}}{\sqrt{32\pi}}(\sin^2(\theta)\cos(\theta)e^{2i\phi}), l = 2, m = 2$



Zonal harmonics can even be applied to seasonal variations in Earth's gravity field [25]. The following graph displays the node residual for the four Starlette 1-year arc between 1998 to 1991.



**6.2. Sectoral Harmonics.** Sectoral harmonics, by contrast are those harmonics with the form  $Y_m^m$  or  $Y_{-m}^{-m}$  [41].

One of the primary applications of sectoral harmonics comes in geodesic equations. Sectoral harmonics define geodesic equations on surface by the Morales-Ramis theorem and Kovacic algorithm [38].

The Geodesic equation [6] states

$$\nabla_{\lambda} T^{\mu} = \frac{dT^{\mu}}{d\lambda} + \Gamma_{\kappa\nu}^{\mu} T^{\nu} \frac{dx^{\kappa}}{d\lambda}$$

Determining the numerical approximation to a geodesic uses the following steps.

- First, we initialize  $\lambda$ ,  $x^{\mu}$ , and  $\frac{dx^{\mu}}{d\lambda}$ .
- We then create a increment,  $\Delta\lambda$  in order to increment  $\lambda$ .
- Then, calculate  $\frac{d^2x^{\mu}}{d\lambda^2}$  for every increment.
- Following this, we add  $\frac{d^2x^{\mu}}{d\lambda^2}\Delta\lambda$  to the value in  $\frac{dx^{\mu}}{d\lambda}$ .
- We then add  $\frac{d^2x^{\mu}}{d\lambda^2}\Delta\lambda$  to the value in  $x^{\mu}$ .
- We then add  $\Delta\lambda$  to the value in  $\lambda$ .
- We will repeat the steps until we get the ideal affine distance.

**6.3. Tesseral Harmonics.** Any harmonic that is neither a sectoral or a zonal harmonic is called a tesseral harmonic [7].

**6.4. Orthogonality of Spherical Harmonics.** In vector calculus, vectors in a set are orthonormal if all the vectors in the set have a magnitude of 1 and are orthogonal to each other. If we integrate the product of two functions  $a(x)$  and  $b(x)$ , we have

$$\int a(x)b(x) dx$$

If we expand this function, now where  $a$  and  $b$  are band-limited functions, we get

$$\int a(x)b(x) dx = \sum_{i=0}^N a_i b_i$$

This type of integration, known as symbolic integration, forms the basis for more complex orthonormality in integrals, such as those used in computer simulations such as Monte Carlo Integration and the Fourier Series [27] [4]. The Fourier series is a clean method of writing periodic functions as sums of sines and cosines [28]. Making use of orthogonality relationships between sines and cosines, the method of harmonics analysis breaks up arbitrary periodic functions to obtain the solution to a Fourier problem [39].

**6.5. Real Spherical Harmonics.** The definition of the spherical harmonics that we saw earlier was based on a more trigonometric basis [29]. Real spherical harmonics, on the other hand, have only one sine. As a result, the normalization factor gets adjusted by  $\sqrt{2}$ .

Real-valued spherical harmonics are defined as

$$(6.1) \quad y_l^m(\theta, \phi) = \begin{cases} \sqrt{2}K_l^m \cos(m\phi) P_l^m(\cos(\theta)) & \text{if } m > 0 \\ K_l^0 P_l^0(\cos(\theta)) & \text{if } m = 0 \\ \sqrt{2}K_l^m \sin(-m\phi) P_l^{-m}(\cos(\theta)) & \text{if } m < 0 \end{cases}$$

Unlike the previous definition for spherical harmonics, which uses two parameters, the real spherical harmonic functions can be reduced to a one dimensional vector[5]. For example, the following function explains this.

$$y_i(\theta, \phi) = y_i^m(\theta, \phi)$$

where  $i = (l + 1)l + m$ .

When it comes to atomic symmetry, real spherical harmonics perform far better than ordinary spherical harmonics [21]. Real spherical harmonics form the basis for electronic-structure calculations. While, ordinary spherical harmonics can be more easily manipulated, they require complex calculations. Real spherical harmonics, on the other hand, require half the computer memory. Cartesian function, just like ordinary spherical harmonics, can be easily manipulated but they result in less atomic symmetry. As a result, real spherical harmonics trump both when atomic symmetry is required [15].

**6.6. Convolution.** A spherical function, namely  $f$ , can be convoluted with a circular symmetric kernel  $k$  (has no  $\phi$  dependence) [33] [33]. By the Funk-Hecke Theorem, which states that surface spherical harmonics are eigen functions of a class of integral operators on the unit two-sphere, where the kernels depend solely on the angle between the vectors [12], we get the following equation

$$(k * f)_l^m = \sqrt{\frac{4\pi}{2l+1}} k_l^0 f_l^m = \alpha_l k_l^0 f_l^m.$$

The Funk-Hecke theorem [3] states that if  $k(u \cdot v)$  is a bounded function over  $[-1,1]$ , then  $k * Y_{nm} = \alpha_n Y_{nm}$  where  $\alpha_n = \sqrt{\frac{4\pi}{2n+1}} k_n$ .

A more formal manner to write the Funk-Hecke theorem is as follows [35].

**Theorem 4.** *If  $\int_{-1}^1 |F(t)|(1-t^2)^{\frac{n-3}{2}} dt < \infty$  and  $S_m \in SH^m$ , where  $SH^m$  is a space of spherical harmonics with degree  $k$  and  $F$  is a homogenous function of degree  $m$  where  $F(tx) = t^m F(x)$  where  $t > 0$ , then for some  $\sigma$  and  $\eta$*

$$\int_{S^{n-1}} F(\langle \sigma, \eta \rangle) S_m(\sigma) d\sigma$$

$$= S_m(\sigma) S^{n-2} C_m(1)^{-1} \int_{-1}^1 |F(t) C_m(t) (1-t^2)^{\frac{n-3}{2}} dt$$

where  $C_m(t)$  is given to be the Gegenbauer polynomial  $C_m^\lambda(t)$  with  $\lambda = \frac{1}{2}n - 1$ .

In essence, the theorem suggests that convoluting a function  $k$  with a spherical harmonic,  $Y_{mn}$ , will result in the same harmonic, multiplied by a scalar  $\alpha_n$ .  $\alpha_n$  varies with  $k$  and is directly related to  $k_n$ , the  $n$ th order coefficient of  $k$ 's harmonic expansion [14].

We can now define a reflectance function  $r$  to be

$$r = k * \ell = \sum_{n=0}^{\infty} \sum_{m=-n}^n (\alpha_n l_{nm}) Y_{nm}$$

We can also derive the harmonic expansion of the Lambertian kernel [13] by getting

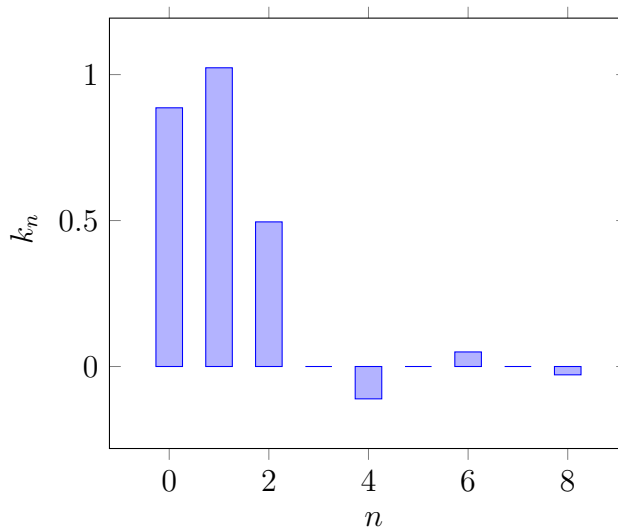
$$(6.2) \quad y_l^m(\theta, \phi) = \begin{cases} \frac{\sqrt{\pi}}{2} & \text{if } n = 0 \\ \sqrt{\frac{\pi}{3}} & \text{if } n = 1 \\ (-1)^{\frac{n+2}{2}} \frac{\sqrt{(2n+1)\pi}}{2^n(n-1)(n+2)} & \text{if } n \geq 2, \text{ even} \\ 0 & \text{if } n \geq 2, \text{ odd} \end{cases}$$

We can obtain the first couple values for  $k_n$  in the following table.

The coefficients approach 0 as  $O(n^{-2})$  as seen in the following graph.

$n$	$k_n$
0	$\frac{\sqrt{\pi}}{2}$
1	$\sqrt{\frac{\pi}{3}}$
2	$\frac{\sqrt{5\pi}}{8}$
3	0
4	$-\frac{\sqrt{\pi}}{16}$
5	0
6	$\frac{\sqrt{13\pi}}{128}$
7	0
8	$\frac{\sqrt{17\pi}}{256}$

**Table 4.** Coefficients of convolution kernel



**6.7. Rotational Invariance of Spherical Harmonics.** A major challenge in shape matching is that a shape and its image under a transformation are considered to be the same [22]. Two solutions, normalization and invariance, are candidates to bring about efficient retrieval.

In normalization, shapes are assumed to be optimally aligned. The amount of similarity for the shape can be found with a much less complex approach rather than attempting to use all the available transformations [24].

Shapes that are defined in an invariant manner, on the other hand, have transformations described in a similar way, but the greatest amount of similarity between the shape and its transformation can be found at any transformation [30].

Rotational invariant descriptor computation for spherical harmonics uses the following methodology:

- Decomposing the spherical function into its individual harmonics.
- Summing the harmonics and determining each frequency.
- Find the norm of each frequency component

Knowing that spherical functions are the sum of their corresponding harmonics, we have the following equation

$$f(\theta, \phi) = \sum_{l=0}^{\infty} \sum_{m=-l}^{m=l} (a_{lm} Y_l^m(\theta, \phi))$$

If we define  $l$  to be the frequency, we can define the subspace to be the following

$$V_l = \text{Span}(Y_l^{-l}, Y_l^{-l+1}, \dots, Y_l^{l-1}, Y_l^l)$$

There are two key notes about  $V_l$ .

- If a function  $f$  and rotation  $R$  exist such that  $f \in V_l$ , the  $R(f) \in V_l$
- $V_l$  cannot be reduced as a direct sum  $V_l = V_l' \oplus V_l''$  ( $V_l'$  and  $V_l''$  are non-trivial representations of the rotation group). If  $f$  is the function of a certain frequency  $l$ , then another function with a frequency of  $l$  can still be expressed as a sum of rotations of  $f$ . As a result, we cannot partition the space of spherical harmonic functions, and rotations exist only in smaller subspaces.

Spherical harmonic representation, however, has key limitations.

When transitioning from a spherical shape to spherical harmonic, representation, information is lost. To illustrate this, if we consider a spherical function  $f(\theta, \phi)$  with bandwidth  $b$ , then we get the following equation

$$f(\theta, \phi) = \sum_{l=0}^b \sum_{m=-l}^l (a_{lm} Y_l^m(\theta, \phi))$$

The space of spherical function with a bandwidth of  $b$  has a dimension  $O(b^2)$ . On the other hand, spherical harmonic representation has a dimension of  $O(b)$ . As a result, nearly a full dimension of information gets lost from going to a spherical function to its harmonic representation. This can happen in two different ways.

We can create frequency components  $f$  and  $g$ , such that

$$f = \sum_{l=0}^b f_l$$

and

$$g = \sum_{l=0}^b R_l(f_l)$$

$R_l$  is defined to be the rotation. The spherical harmonic representation does not change with different rotations or frequencies.

Furthermore, every frequency component,  $f_l$ , the spherical harmonic representation will only store the energy for that component.

## 7. APPLICATIONS OF SPHERICAL HARMONICS

With an understanding of spherical harmonics, we can now move to studying the applications of harmonics. Spherical harmonics are used extensively in computer graphics: irradiance environment maps, object recognition, and image relighting.

**7.1. Irradiance Environment Maps.** An environment map is used mainly to store a lighting distribution, namely  $L$  [31]. The object being lighted will have no changes in lighting, and all points on the surface of the object will be equally lit.

Using a normal vector  $\vec{n}$ , we can determine the light at a particular point. This determination depends on integrating the upper hemisphere  $\Omega(\vec{n})$ .

The light model is said to be lambertian and is defined as

$$\int_{\Omega(\vec{n})} L(\omega)(\vec{n} \cdot \omega) d\omega = L * A(\vec{n}) = E(\vec{n})$$

$E(\vec{n})$  is the surface irradiance [31]. In essence, an environmental map maps a normal vector  $\vec{n}$  to  $E(\vec{n})$ .

In addition, the following theorem generalizes incoming distant illumination on convex-curved Lambertian surfaces.

**Theorem 5.** *It is not possible to recover odd-order spherical harmonic modes, with an order greater than 1, from information about the irradiance at every surface point. Observing a convex-curved Lambertian surface still does not determine the odd-order modes (order greater than 1) of an incoming illumination field.*

This approach, however, can be simplified with the use of spherical harmonics in frequency space.

We first define the light function as

$$L(\theta, \phi) = \sum L_l^m Y_l^m(\theta, \phi)$$

When  $m = 0$  and  $\max(\vec{n} \cdot \omega_1, 0) = \max(\cos(\theta), 0)$  is the circular symmetric kernel function, we have

$$A(\vec{n}) = \max(\cos(\theta), 0) = \sum A_l Y_l^0(\vec{n})$$

and we can rewrite  $E(\vec{n})$  to be

$$E(\vec{n}) = \sum \alpha_l A_l L_l^m Y_l^m(\vec{n})$$

When we write down the first 9 spherical harmonics in Cartesian coordinates, we notice that this computation can be performed easily on a modern fragment or vertex shader hardware by solving the following polynomial equation [32].

$$E(x, y, z) = \sum_{l=0}^2 \sum_{m=-1}^l \alpha_l A_l L_l^m Y_l^m(x, y, z)$$

$$= c_1 L_2^2(x^2 - y^2) + c_3 L_2^0 z^2 - c_5 L_2^0 + c_4 L_0^0 + 2c_1(L_2^{-2}xy + L_2^1xz + L_2^{-1}yz) + 2c_2(L_1^1x + L_1^{-1}y + L_1^0z)$$

Solving the constants we get

$$c_1 = 0.429043$$

$$c_2 = 0.511664$$

$$c_3 = 0.743125$$

$$c_4 = 0.886227$$

$$c_5 = 0.247708$$

Spherical harmonic coefficients can be computed, which significantly brings down the time for a scalar product of the vertex's normal and irradiance components [1]. Furthermore, this illustrates the aforementioned property that a spherical function can be decomposed into the sum of its harmonics.

One of the most interesting applications of spherical harmonics in irradiance environment maps comes in control variate sampling to render images. As seen in the following figure, spherical harmonics control variate sampling allows one of render the production of fur.

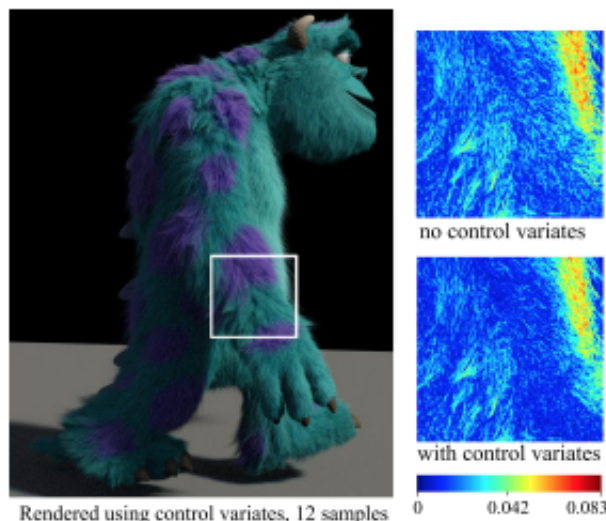


**Figure 12.** Image copyright (2012) Pixar. All Rights Reserved.

We can also create tangent irradiance maps, which use tangent data from real datasets. In Figure 13, image (a) shows the visualization of tangent fields corresponds to polar angles on the figure's plane. These tangents lie in concentric circles. Images (b) and (c) are constant along the radial lines from the center. In Figure 13, we use a real object to apply tangents. This, in fact, allows one to visualize the object with realistic tangents in an environment map.

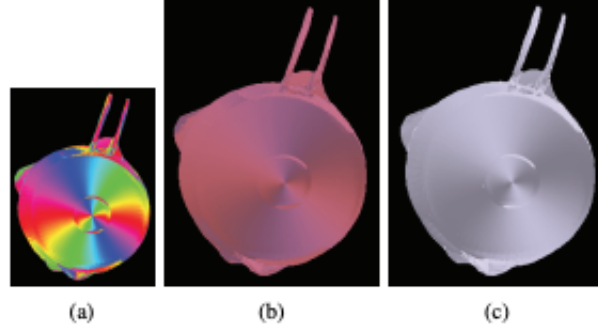


**Figure 13.** Image copyright *Analytic Tangent Irradiance Environment Maps for Anisotropic Surfaces*

**7.2. Spherical Harmonics in Computer Graphics.** While irradiance heat maps provide a strong baseline for computer graphics, spherical harmonic lighting is one method that performs dynamic illumination with a high degree of efficiency.

The foundation of spherical harmonic lighting is the rendering equation.

The rendering equation states

$$L(x, \omega_v) = L_e(x, \omega_v) + \int_S R(x, -\omega, \omega_v) L(x_\omega, -\omega) G(x, x_\omega) V(x, x_\omega) d\omega.$$

$L_e(x, \omega_v)$  is the light emitted by a point  $x$  in the direction  $\omega_v$ , without the influence of any other incident light ray. The function  $G(x, x')$  describes how its two parameters are related to one another.  $x'$  is a point in the direction  $\omega$  from  $x$ .  $V(x, x')$  is the visibility relationship between two points, measured by 0 or 1.

A new algorithm has been developed to divide the rendering equation into a light source function, denoted by  $L^I$ . This is given as follows

$$L(x, \omega_v) = L_e(x, \omega_v) + \int_S L^I(x, -\omega, \omega_v) T(x, -\omega, \omega_v) d\omega.$$

The transfer function  $T(x, -\omega, \omega_v)$  provides a measure of how light from  $L^I$  is redirected in the direction  $\omega_v$ .

The previous equation describes the intensity when rendering a point on its surface [23] [11]. Because these functions are based on spherical harmonics, the new equation for diffuse is

$$L(x, \omega_v) = L_e(x, \omega_v) + \sum_i L_i^I T_i$$

and for view dependent light models, the equation is

$$L(x, \omega_v) = L_e(x, \omega_v) + \sum_i \alpha_i R_i \left( \sum_j T_{ij} L_j^I \right) y^i(\omega_v)$$



$\sum_j T_{ij} L_j^I$  is the linear transformation of the light coefficient by the transfer function [18] [36].

## 8. CONCLUSION

This paper gives a brief overview of spherical harmonics and their applications. These harmonics, while complicated, provide a baseline for more complicated spherical functions. Spherical harmonics have a plethora of application extending from computer graphics to transfer functions.

## 9. ACKNOWLEDGEMENTS

The author of this paper would like to thank his mentor, Alex Perry for providing critical support during the research and writing phases of this paper. Gratitude is also extended to the Euler Circle and Dr. Simon Rubinstein-Salzedo, who provided the platform necessary to conduct this project.

## REFERENCES

- [1] Sameer Agarwal et al. “Structured importance sampling of environment maps”. In: *ACM SIGGRAPH 2003 Papers*. 2003, pp. 605–612.
- [2] Rubén G Barrera, GA Estevez, and J Giraldo. “Vector spherical harmonics and their application to magnetostatics”. In: *European Journal of Physics* 6.4 (1985), p. 287.
- [3] Ronen Basri and David W Jacobs. “Lambertian reflectance and linear subspaces”. In: *IEEE transactions on pattern analysis and machine intelligence* 25.2 (2003), pp. 218–233.
- [4] Manuel Bronstein. *Symbolic integration I: transcendental functions*. Vol. 1. Springer Science & Business Media, 2005.
- [5] JoséRamón Álvarez Collado et al. “Rotation of real spherical harmonics”. In: *Computer physics communications* 52.3 (1989), pp. 323–331.
- [6] Benjamin Crowell. “5.8: The Geodesic Equation”. In: *Libre Texts: Physics* ().
- [7] Pawel Danielewicz and Scott Pratt. “Analyzing correlation functions with tesseral and Cartesian spherical harmonics”. In: *Physical Review C* 75.3 (2007), p. 034907.
- [8] B Davison. “Spherical-harmonics method for neutron transport theory problems with incomplete symmetry”. In: *Canadian Journal of Physics* 36.4 (1958), pp. 462–475.
- [9] Hendrik De Bie, David Eelbode, and Franciscus Sommen. “Spherical harmonics and integration in superspace: II”. In: *Journal of Physics A: Mathematical and Theoretical* 42.24 (2009), p. 245204.
- [10] Hendrik De Bie and Frank Sommen. “Spherical harmonics and integration in superspace”. In: *Journal of Physics A: Mathematical and Theoretical* 40.26 (2007), p. 7193.
- [11] Yoshinori Dobashi et al. “A quick rendering method using basis functions for interactive lighting design”. In: *Computer Graphics Forum*. Vol. 14. 3. Wiley Online Library. 1995, pp. 229–240.
- [12] JS Dowker. “A discrete Funk-Hecke theorem”. In: *arXiv preprint arXiv:2303.05362* (2023).
- [13] Shireen Y Elhabian, Ham Rara, and Aly A Farag. “Towards accurate and efficient representation of image irradiance of convex-Lambertian objects under unknown near lighting”. In: *2011 International Conference on Computer Vision*. IEEE. 2011, pp. 1732–1737.

- [14] Zhiying Fang et al. “Theory of deep convolutional neural networks II: Spherical analysis”. In: *Neural Networks* 131 (2020), pp. 154–162.
- [15] HA Fertig and W Kohn. “Symmetry of the atomic electron density in Hartree, Hartree-Fock, and density-functional theories”. In: *Physical Review A* 62.5 (2000), p. 052511.
- [16] Walter W Funkenbusch. “From Euler’s formula to Pick’s formula using an Edge theorem”. In: *The American Mathematical Monthly* 81.6 (1974), pp. 647–648.
- [17] Henry W Gould. “Euler’s formula for  $n$  th differences of powers”. In: *The American Mathematical Monthly* 85.6 (1978), pp. 450–467.
- [18] Robin Green. “Spherical harmonic lighting: The gritty details”. In: *Archives of the game developers conference*. Vol. 56. 2003, p. 4.
- [19] Helmut Groemer. *Geometric applications of Fourier series and spherical harmonics*. Vol. 61. Cambridge University Press, 1996.
- [20] EL Hill. “The theory of vector spherical harmonics”. In: *American Journal of Physics* 22.4 (1954), pp. 211–214.
- [21] Qinghua Huang, Lin Zhang, and Yong Fang. “Two-stage decoupled DOA estimation based on real spherical harmonics for spherical arrays”. In: *IEEE/ACM Transactions on Audio, Speech, and Language Processing* 25.11 (2017), pp. 2045–2058.
- [22] Michael Kazhdan, Thomas Funkhouser, and Szymon Rusinkiewicz. “Rotation invariant spherical harmonic representation of 3 d shape descriptors”. In: *Symposium on geometry processing*. Vol. 6. 2003, pp. 156–164.
- [23] Clifford Lindsay and Emmanuel Agu. “Physically-based real-time diffraction using spherical harmonics”. In: *International Symposium on Visual Computing*. Springer. 2006, pp. 505–517.
- [24] Lora Mak, Scott Grandison, and Richard J Morris. “An extension of spherical harmonics to region-based rotationally invariant descriptors for molecular shape description and comparison”. In: *Journal of Molecular Graphics and Modelling* 26.7 (2008), pp. 1035–1045.
- [25] Vladimir Martinuši and Pini Gurfil. “Solutions and periodicity of satellite relative motion under even zonal harmonics perturbations”. In: *Celestial Mechanics and Dynamical Astronomy* 111 (2011), pp. 387–414.
- [26] Martin J Mohlenkamp. “A fast transform for spherical harmonics”. In: *Journal of Fourier analysis and applications* 5 (1999), pp. 159–184.
- [27] Joel Moses. “Symbolic integration”. In: (1967).
- [28] Joel Moses. “Symbolic integration: The stormy decade”. In: *Communications of the ACM* 14.8 (1971), pp. 548–560.
- [29] Didier Pinchon and Philip E Hoggan. “Rotation matrices for real spherical harmonics: general rotations of atomic orbitals in space-fixed axes”. In: *Journal of Physics A: Mathematical and Theoretical* 40.7 (2007), p. 1597.
- [30] Adrien Poulenard et al. “Effective rotation-invariant point cnn with spherical harmonics kernels”. In: *2019 International Conference on 3D Vision (3DV)*. IEEE. 2019, pp. 47–56.
- [31] Ravi Ramamoorthi and Pat Hanrahan. “An efficient representation for irradiance environment maps”. In: *Proceedings of the 28th annual conference on Computer graphics and interactive techniques*. 2001, pp. 497–500.

- [32] Ravi Ramamoorthi and Pat Hanrahan. “Frequency space environment map rendering”. In: *Proceedings of the 29th annual conference on Computer graphics and interactive techniques*. 2002, pp. 517–526.
- [33] Patrick J Roddy and Jason D McEwen. “Sifting convolution on the sphere”. In: *IEEE Signal Processing Letters* 28 (2021), pp. 304–308.
- [34] Volker Schönefeld. “Spherical harmonics”. In: *Computer Graphics and Multimedia Group, Technical Note. RWTH Aachen University, Germany* (2005), p. 18.
- [35] Robert T Seeley. “Spherical harmonics”. In: *The American Mathematical Monthly* 73.4P2 (1966), pp. 115–121.
- [36] Peter-Pike Sloan, Jan Kautz, and John Snyder. “Precomputed radiance transfer for real-time rendering in dynamic, low-frequency lighting environments”. In: *Proceedings of the 29th annual conference on Computer graphics and interactive techniques*. 2002, pp. 527–536.
- [37] James Joseph Sylvester. “XXXVII. Note on spherical harmonics”. In: *The London, Edinburgh, and Dublin Philosophical Magazine and Journal of Science* 2.11 (1876), pp. 291–307.
- [38] Thomas J Waters. “Regular and irregular geodesics on spherical harmonic surfaces”. In: *Physica D: Nonlinear Phenomena* 241.5 (2012), pp. 543–552.
- [39] Eric W. Weisstein. “Fourier Series”. In: *MathWorld* ().
- [40] Eric W. Weisstein. “Spherical Harmonic”. In: *MathWorld* ().
- [41] Mark A Wiczorek and Matthias Meschede. “SHTools: Tools for working with spherical harmonics”. In: *Geochemistry, Geophysics, Geosystems* 19.8 (2018), pp. 2574–2592.
- [42] Bert Wouters and Ernst JO Schrama. “Improved accuracy of GRACE gravity solutions through empirical orthogonal function filtering of spherical harmonics”. In: *Geophysical Research Letters* 34.23 (2007).

EULER CIRCLE, MOUNTAIN VIEW, CA 94040  
Email address: vjanapaty5@gmail.com